J Mater Sci: Mater Med (2006) 17:979–987
DOI 10.1007/s10856-006-0433-y

The surface functionalization of 45S5 Bioglass®-based glass-ceramic scaffolds and its impact on bioactivity

Q. Z. Chen · K. Rezwan · D. Armitage · S. N. Nazhat · A. R. Boccaccini

Received: 25 October 2005 / Accepted: 27 February 2006

Abstract The first and foremost function of a tissue engineering scaffold is its role as a substrate for cell attachment, and their subsequent growth and proliferation. However, cells do not attach directly to the culture substrate; rather they bind to proteins that are adsorbed to the scaffold's surface. Like standard tissue culture plates, tissue engineering scaffolds can be chemically treated to couple proteins without losing the conformational functionality; a process called *surface functionalization*. In this work, novel highly porous 45S5 Bioglass®-based scaffolds have been functionalized applying 3-AminoPropyl-TriethoxySilane (APTS) and glutaraldehyde (GA) without the use of organic solvents. The efficiency and stability of the surface modification was assessed by X-ray photoemission spectroscopy (XPS). The bioactivity of the functionalized scaffolds was investigated using simulated body fluid (SBF) and characterized by scanning electron microscopy (SEM), energy dispersive spectroscopy (EDS) and X-ray diffraction (XRD). It was found that the aqueous heat-treatment applied at 80°C for 4 hrs during the surface functionalization procedure accelerated the structural transition of the crystalline $Na_2Ca_2Si_3O_9$ phase, present in the original scaffold structure as a result of the sintering process used for fabrication, to an amorphous phase during SBF immersion. The surface functionalized scaffolds exhibited an accelerated crystalline hydroxyapatite layer formation upon immersion in SBF caused by ion leaching and the increased surface roughness induced during the heat treatment step. The possible mechanisms behind this phenomenon are discussed.

Q. Z Chen and K. Rezwan both authors contributed equally to this work.

Q. Z. Chen · K. Rezwan · A. R. Boccaccini (✉)
Department of Materials, Imperial College London,
Prince Consort Road, London SW7 2BP, UK
e-mail: a.boccaccini@imperial.ac.uk

D. Armitage · S. N. Nazhat
Biomaterials and Tissue Engineering,
UCL Eastman Dental Institute,
256 Gray's Inn Road, London, WC1X 8LD, UK

1 Introduction

Protein adsorption on surfaces of biomaterials and medical implants is an essential aspect of the cascade of biological reactions taking place at the interface between a synthetic material and the biological environment. Type, amount and conformation of adsorbed proteins mediate subsequent adhesion, proliferation and differentiation of cells and they are believed to steer foreign body response and inflammatory processes [1–3]. Protein signaling regulates cell phenotype and thus tissue structure and function. Biomaterial vehicles are being designed to incorporate and locally deliver various molecules involved in this signaling, including both growth factors and peptides that mimic whole proteins [4]. Controlling the concentration, local duration and spatial distribution of these factors is the key to their utility and efficacy. A promising strategy being extensively investigated is the encapsulation of growth factors or collagen in biodegradable polymer matrices that release over time the incorporated biomolecules [5–15]. However, there has been much less research and development efforts on designing strategies to load inorganic substrates, e.g. ceramics and glasses, with biomolecules. Loading of ceramic scaffolds can be carried out without using any coupling agents [16]. It is known however that under such conditions electrostatic and hydrophobic interactions are dominant [17–20] and that conformational changes of the native biomolecule structure may occur [21–23].

To load ceramic substrates with proteins, several protein immobilization techniques are being applied in biosensor research. The use of protein coupling agents allows the control of protein release kinetics and maintains almost completely the native protein structure [24–27]. One common approach is to firstly silanize the ceramic surface with a sol–gel precursor, followed by the attachment of a protein coupling agent such as glutaraldehyde (GA) [24, 28]. Glutaraldehyde is known to be cytotoxic if not bound and it can be replaced by other coupling agents such as genipin for *in vitro* and *in vivo* studies [29]. Protein release kinetic studies for sol–gel derived bioactive foams (70S30C and ternary 58S compositions) have been carried out in a previous study [30]. However, the silanization process was performed without using a protein coupling agent and organic solvents were used, which are not ideal for biocompatibility reasons.

In this study highly porous 45S5 Bioglass®-based scaffolds fabricated by the polymer replica technique [31], which are intended for bone tissue engineering applications [32], have been surface functionalized. Silanization was realized at 80°C for 4 hrs in an aqueous solution. The effect of the elevated processing temperature and the impact of the applied organic molecules on hydroxyapatite (HA) formation in simulated body fluid (SBF) was investigated and characterized. GA is used as a model protein coupling agent. GA was chosen primarily as a model system because it has been successfully used in biosensor applications, it is readily available and it has low-cost. The surface functionalized Bioglass®-based scaffolds are being developed for collagen, growth factor and antibiotic immobilization for applications in the field of bone tissue engineering with the aim to elucidate cell reactions to protein loaded bioactive materials.

2 Experimental

2.1 Materials

Melt derived 45S5 Bioglass® powder (gift of Dr. I. Thompson, King's College London, UK) was ball-milled to a particle size of 5–10 microns as found by SEM image analysis. Poly vinyl alcohol (PVA, 98–99% hydrolyzed, 363154), 3-aminopropyl-triethoxysilane (APTS, 99%, 440140) and glutaraldehyde (GA, 2.6 M in water, 49630) were purchased from Sigma Aldrich and Fluka. For preparation of Bioglass®-based scaffolds by the replica technique [31] fully reticulated polyurethane foam with 60 ppi (pores per inch) from Recticel UK (Corby) was applied in this study. Double deionised water with an electrical resistance of >18 MΩcm was used for all experiments.

2.2 Methods

2.2.1 Scaffold and pellet fabrication

Porous, highly interconnected 3D Bioglass® scaffolds were fabricated by using the polymer replica method as described in detail elsewhere [32]. An aqueous solution of PVA with a concentration of 0.1 mol/L was prepared and Bioglass® powder added under vigorous stirring to a total of 40 wt% solid content. After 1 h of stirring, a polyurethane foam sample with dimension $10 \times 10 \times 10$ mm^3 was immersed in the Bioglass® suspension for 15 min. Subsequently, the foam was taken out and squeezed, removing the excess of slurry. The sample was dried for 12 hrs at ambient conditions and afterwards sintered at 1000°C for 1 h.

For determination of the effectiveness of the functionalisation procedure by XPS, cylindrical Bioglass® pellets were fabricated by pressing and sintering powders. A quantity of 0.3 g Bioglass® powder was cold-pressed into cylindrical pellets of 8 mm radius/2 mm thickness and sintered at the same conditions used for fabrication of the porous scaffolds. These samples were used for X-ray photoemission spectroscopy (XPS) analysis, as discussed below.

2.2.2 Surface functionalization

The scaffold and pellet samples were surface functionalized by adapting the protocols from previous studies [24, 27]. An aqueous APTS solution of 0.45 mol/L was prepared and the pH adjusted to 8 by addition of 1 N HCl, resulting in a total volume of 70 ml. The samples to be functionalized were immersed into the obtained aqueous solution, contained in a glass bottle with the lid fastened. The solution was heated up to 80°C in an oil bath under stirring conditions. After 4 hrs the samples were taken out and cleaned for 5 min in 300 ml of deionised water. The samples were subsequently dried and immersed for 1 h in a 50 ml GA solution (1 mol/L) at ambient conditions. Finally, the surface functionalized samples were cleaned again in deionised water and dried at ambient conditions. Control samples were prepared in exactly the same way but without using APTS and GA. They were only heat-treated at 80°C for 4 hrs at pH 8. These control samples are referred to as "heat-treated" samples throughout the text.

2.2.3 Study of bioactivity in simulated body fluid (SBF)

The standard procedure by Kokubo et al. [33] was applied to investigate hydroxyapatite (HA) formation in Simulated Body Fluid (SBF). It is established [34–36] that HA formation on materials surfaces upon immersion in SBF is an indication of the bioactivity of a material. The SBF composition was taken from ref. [35]. Each sample was immersed in 75 ml of acellular SBF in sterilized conical polypropylene

flasks. The flasks with fastened lids were placed into an incubator at a constant temperature of 37°C. After 3 days and 1 week samples were withdrawn, rinsed and dried at ambient conditions for characterization. The SBF solution was completely replaced every three days. Three set of samples, both porous scaffolds and dense pellets, were investigated: as-fabricated, heat-treated and surface functionalized.

2.3 Characterization

2.3.1 X-ray photoemission spectroscopy (XPS)

Surface analysis of control and modified pellet surfaces was performed using an ESCALAB 200i-XL spectrometer operated in large area XL magnetic lens mode with a monochromatic AlK_α X-ray source (1 mm^2 spot size). Charge compensation was carried out using an electron flood gun. The system pressure was below 5×10^{-8} mbar. The take-off angle was maintained at 0° to the surface normal. Survey spectra were collected at a pass energy of 100 eV and detailed spectra at 20 eV. Quantification was performed using Eclipse software (Thermo Electron Corporation) with Schofield sensitivity factors following subtraction of linear backgrounds.

2.3.2 Scanning electron microscopy (SEM) and energy dispersive spectroscopy (EDS)

The microstructures of Bioglass®-based foams were characterized in a LEO Gemini SEM, before and after immersion in simulated body fluid (SBF). Samples were gold-sputtered and observed at accelerating voltages of 15–20 kV. Energy dispersive X-ray spectra (K_α line) of scaffold surface areas of 1×1 μm^2were recorded at 20 kV in the field emission gun SEM (FEG-SEM). The spectra were processed by "INCA" (Oxford instruments) software, using standard reference spectra.

2.3.3 X-ray diffraction (XRD)

Scaffold samples before and after immersion in SBF were manually ground to powder and 0.05 g used for XRD analysis (Philips PW 1700 Series). The samples were run with a Cu-K_α source at 40 kV and 40 mA with a secondary crystal monochromator. Data were collected over a range of $2\theta = 5$–80° using a step size of 0.04° and a counting time of 25 s per step.

3 Results

3.1 XPS

XPS analysis was carried out before and after functionalization on sintered pellets to determine the surface compositions with a typical analysis depth of 5–10 nm. In addition, the surfaces were analyzed by XPS after 3 days immersion in SBF. It was assumed that the results of planar sintered pellets would be directly applicable to the scaffold samples fabricated under the same conditions since exactly the same process parameters were used in the functionalization steps.

The results of XPS analysis on samples before and after (3 days) immersion in SBF are shown in Table 1. The detected relatively high concentration of C atoms and non zero concentration of N in the as-fabricated samples are the result of organic contamination on the sintered Bioglass®surface. As mentioned above, XPS measures chemistry to a 10 nm depth, and its sensitivity increases exponentially towards the surface. Organic contamination is a common problem in many systems analysed by XPS. Although the samples were washed with water before testing, the use of solvents was considered inappropriate as possible uncontrolled modifications to the Bioglass® surface were to be avoided. The presence of a carbon layer in the as-fabricated material also accounts for the relatively low silicon signal measured. The carbon layer covers the Bioglass® surface and hence reduces the relative Si concentration in the surface region. On surface modification, increases in carbon, silicon and nitrogen were detected, as expected, since APTS includes these three elements. Although one may expect the surface carbon concentration to increase significantly on modification this is not necessarily true. It appears that the APTS is replacing the organic contamination on the surface. Considering the contributions from Ca and P, for example, it is seen that these decrease considerably; while the silicon concentration increases. This shows that the majority of the silicon signal in the surface modified sample is not from the Bioglass® substrate, but from the APTS.

Table 1 Surface composition (in at.%) obtained by XPS for sintered Bioglass® pellets with and without surface functionalization, before and after immersion in simulated body fluid (SBF) for 3 days

Dataset	Na 1s %	Ca 2p %	P 2p %	O 1s %	C 1s %	Si 2p %	N 1s %
Control (as fabricated)	0.879537	4.6292	4.0255	24.7671	49.5633	14.1324	2.00302
Surface modified	0.298178	0.444443	0.250483	25.1617	51.0736	20.2236	2.54809
Control (as fabricated) after immersion in SBF	1.40865	11.268	10.3354	45.6459	18.4341	11.584	1.32385
Surface modified after immersion in SBF	0.986561	3.43692	3.93279	37.4539	29.9473	19.9621	4.28032

The direct comparison of the reference pellets with the surface modified samples before SBF immersion reveals also deficiency of Na. The O content does not change significantly whereas, as mentioned above, the C content increases slightly due to the original organic impurities on the reference sample. The Si fraction increases in about 50% compared to the unmodified reference.

Results after 3 days immersion in SBF also presented in Table 1 show a consistent increase of Na, Ca, P and O contents for the reference and the modified samples. The total amounts of Na, Ca, P and O are lower, however, for the modified than for the reference sample. For both samples the C content decreases after SBF soaking whereas the Si content stays approximately the same in the functionalised sample but reduces in about 3 at% in the as-fabricated sample.

3.2 SEM and EDS

Figures 1 to 3 show SEM micrographs of the investigated scaffolds after different treatments. Figures 1(a) to (c) show SEM micrographs of as-fabricated scaffolds before and after 3 days and 1 week immersion in SBF. An overview picture of an as-fabricated scaffold at a lower magnification is presented in Fig. 1(d), illustrating the highly interconnected pore structure with pore sizes around 500 μm and a porosity of around 90 vol%, achieved by the replica technique [31, 32]. The as-fabricated scaffold, used as reference in this study, shows little calcium phosphate deposition on the surface after 3 days and 1 week immersion in SBF as illustrated in Fig. 1(b) and 1(c), and discussed elsewhere [32].

Figures 2(a) and 3(a) represent the surfaces of the heat-treated (80°C in aqueous solution for 4 hrs) and surface modified samples before immersion in SBF, respectively. The heat-treated and surface modified samples feature a surface roughness at the microscale as opposed to the reference sample in Fig. 1(a). After 3 days and 1 week of SBF immersion the heat-treated and surface modified samples are almost fully covered with calcium phosphate depositions (Figs. 2(b) and 2(c) and Figs. 3(b) and 3(c)).

Results from EDS analysis are presented in Figs. 4(a)–(h), which show, from left to right, the concentration of relevant elements on scaffold surfaces, as measured before, after 3 days and after 1 week of immersion in SBF. The dotted lines in the graphs represent the reference EDS analysis of a 45S5 Bioglass® scaffold, just after sintering before SBF immersion. The solid lines represent the theoretical composition of stoichiometric HA ($Ca_{10}(PO_4)_6(OH)_2$) with a corresponding Ca to P ratio of 1.67. Before SBF immersion the heat-treated and the surface modified samples show a deficiency in Na

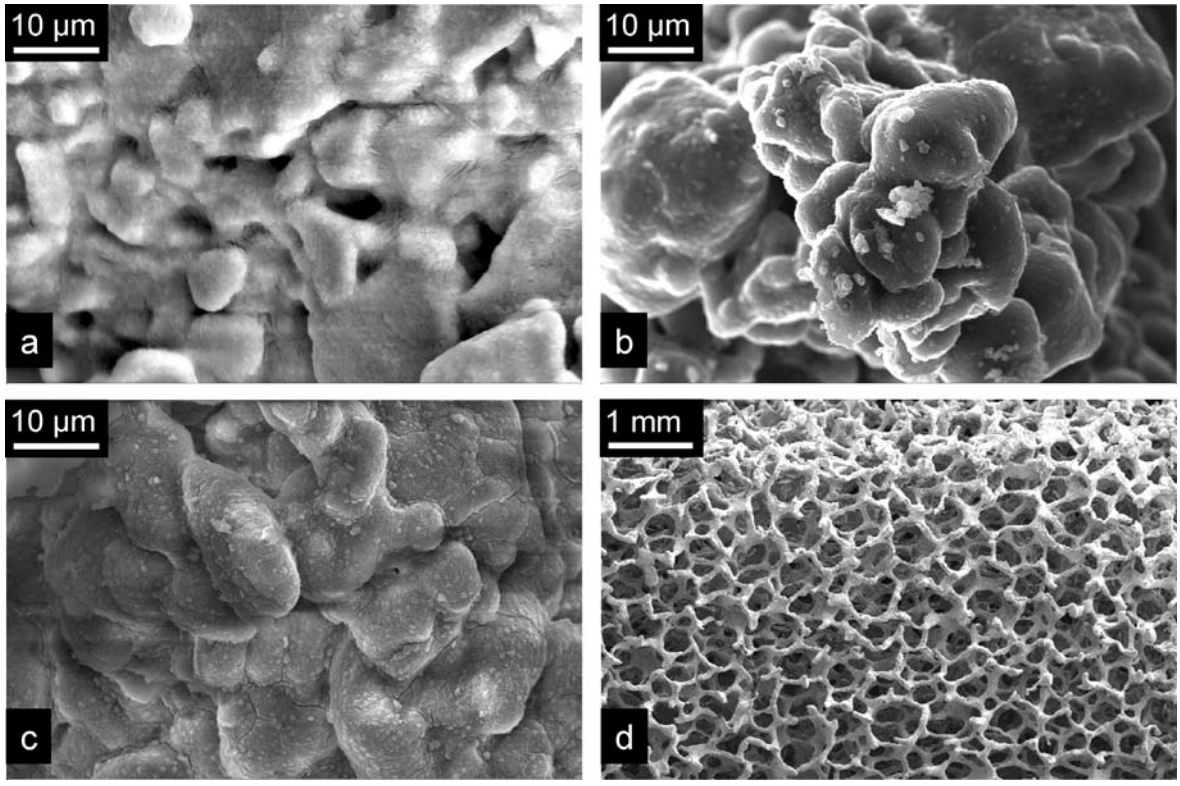

Fig. 1 SEM micrographs of non-modified sintered Bioglass® scaffolds before immersion in SBF (a), after 3 days in SBF (b) and after 1 week in SBF (c). The image in (d) shows the as-fabricated scaffold structure at a lower magnification, indicating the high, uniform porosity achieved by the replica technique [31, 32].

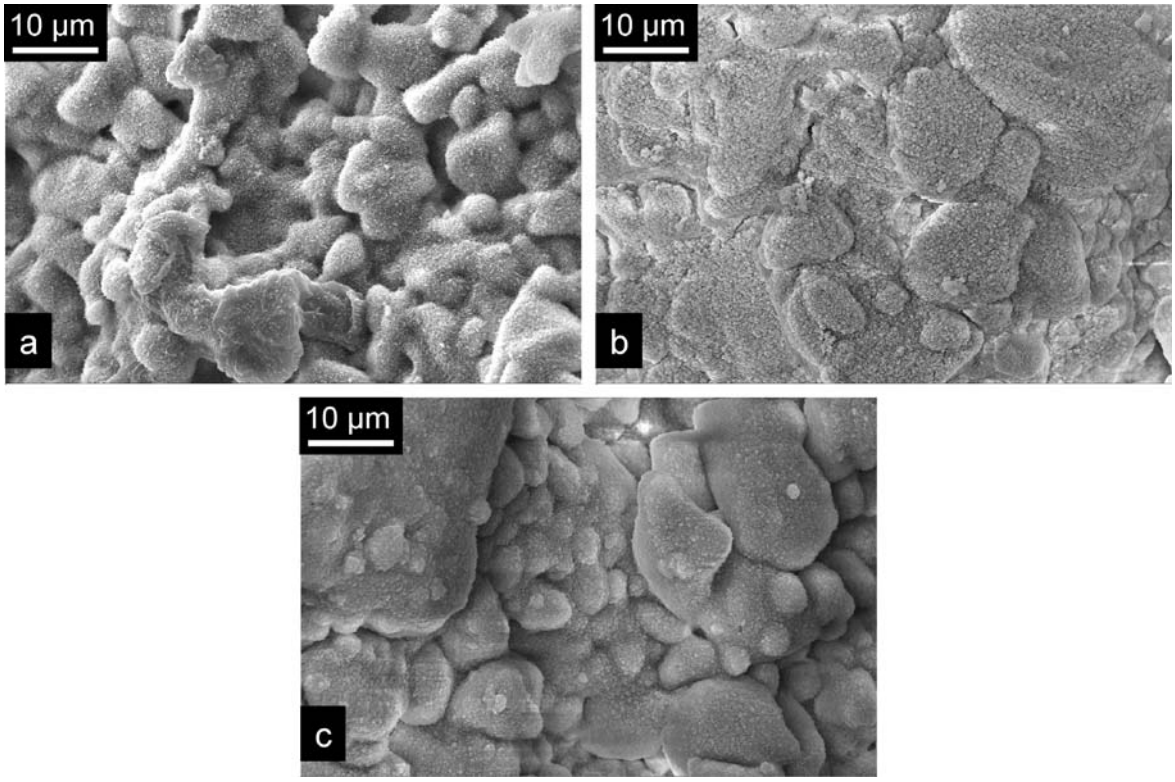

Fig. 2 SEM micrographs of sintered and heat-treated (80°C in aqueous solution for 4 hrs) Bioglass® scaffolds before immersion in SBF (a), after 3 days in SBF (b) and 1 week in SBF (c). A distinct surface roughness is observed on the sample in (a), which is thought to be the result of microporosity induced by ion leaching during heat-treatment in water at 80°C.

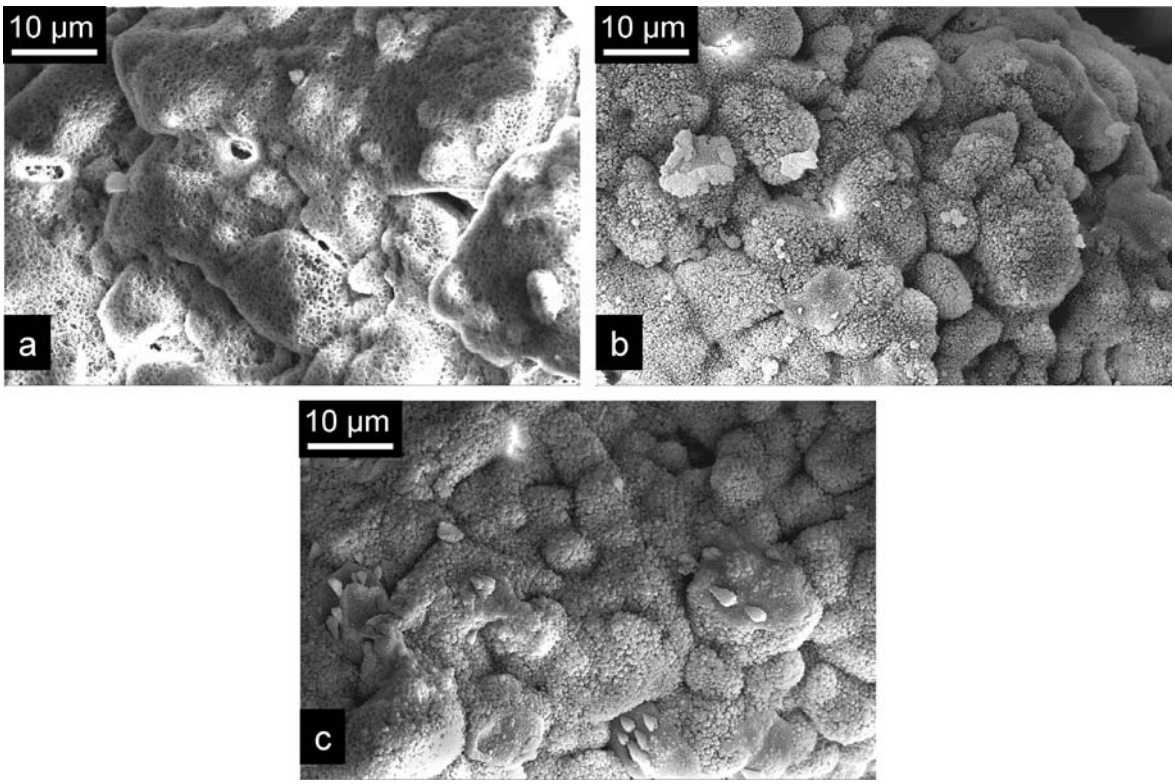

Fig. 3 SEM micrographs of sintered and surface functionalized Bioglass® scaffolds before immersion in SBF (a), after 3 days in SBF (b) and after 1 week in SBF (c). A distinct surface roughness is observed on the sample in (a), which is thought to be the result of microporosity induced by ion leaching during the heat-treatment in water at 80°C.

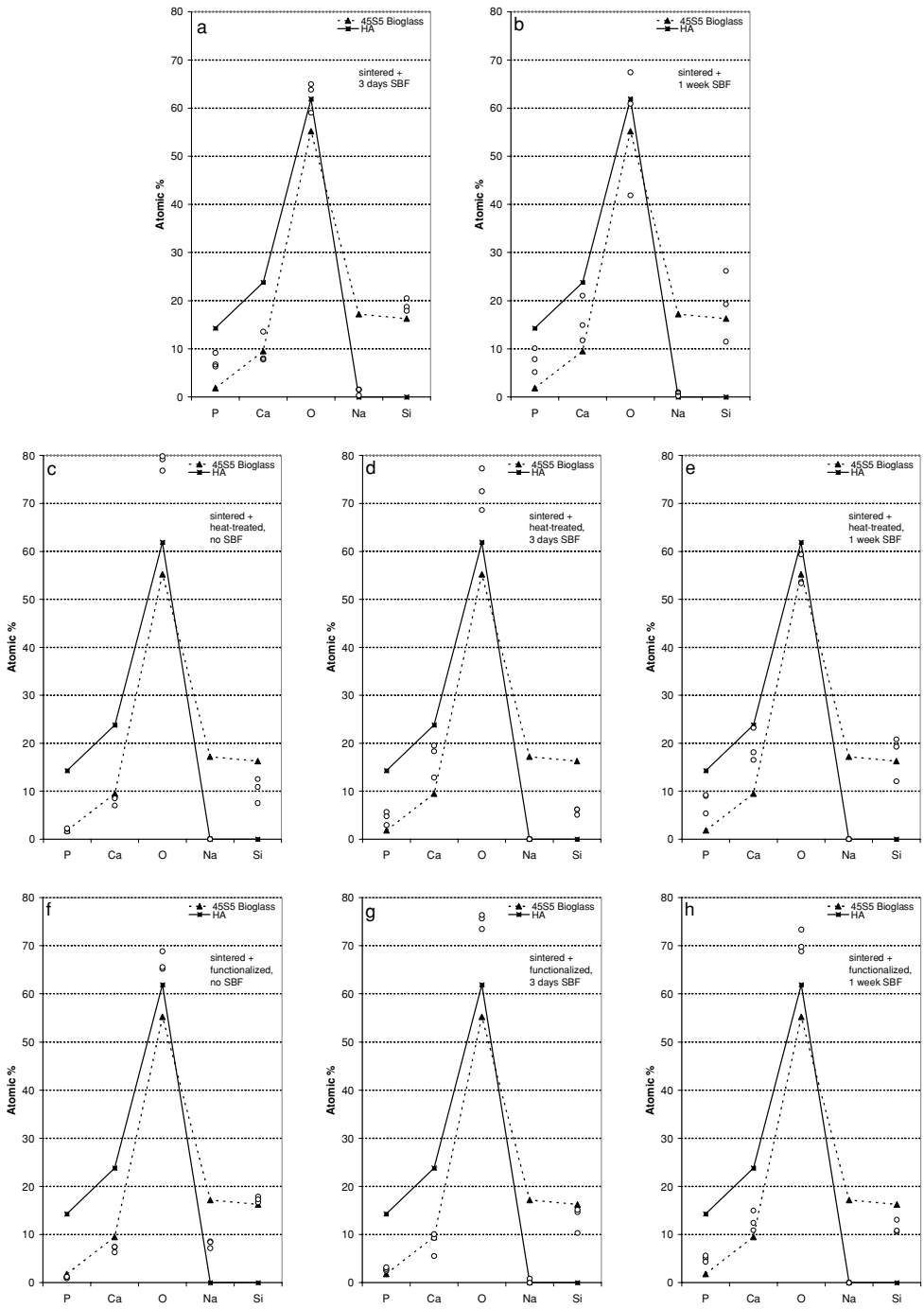

Fig. 4 EDS analysis of scaffolds: (a), (b) sintered after 3 days and 1 week in SBF, respectively. Plots (c)–(e) are sintered and heat-treated scaffolds before immersion in SBF, after 3 days and after 1 week in SBF, respectively, and (f)–(h) sintered and functionalized before immersion in SBF, and after 3 days and 1 week in SBF, respectively. The dotted line represents the reference 45S5 Bioglass® composition and the solid line the theoretical composition of HA with a Ca to P ratio of 1.67.

whereas the reference sample exhibits the same deficiency only after 3 days immersion in SBF. The Si, Ca and P fractions of all samples begin to scatter after 3 days, indicating compositional heterogeneities. After 1 week in SBF all samples show significant increases in the Ca and P contents, as expected, due to the formation of calcium phosphate layers, as observed by SEM (Figs. 1–3). It should be noted, however, that the penetration depth of the EDS analysis at the applied conditions is about 2–5 μm, hence the results also include bulk composition data and therefore no quantitative information on the exact composition of the calcium phosphate layer can be drawn from the presented results.

3.3 XRD

Figure 5 shows the obtained XRD spectra for all investigated samples. The "as-received powder" graphs represent the results for amorphous 45S5 Bioglass® powder in as-received conditions. The diffusive peak at around $2\theta = 27^\circ$ is caused

by the short range ordering of the silicate structure in glasses [36].

All samples, with and without surface modification, exhibit sharp diffraction peaks after sintering. These peaks can be identified as crystallites of a $Na_2Ca_2Si_3O_9$ phase (marked with triangles) using the standard PDF #22.1455. The same crystalline phase has been reported in previous studies on sintered 45S5 Bioglass® powders [31, 37]. After 3 days in SBF the reference sample (Fig. 5(a)) shows a small reduction of crystallinity and a small HA peak (marked with solid squares). Remarkably, the heat-treated and surface modified samples do not feature any remaining crystalline phase ($Na_2Ca_2Si_3O_9$) after 3 days in SBF but pronounced peaks of HA are detected (Figs. 5(b) and (c)). The XRD spectra taken after 3 days and 1 week of SBF immersion do not exhibit any changes, indicating no further structural changes for all investigated samples.

4 Discussion

4.1 Surface functionalization

The XPS analysis of the sintered non-modified and modified Bioglass® pellets presented in Table 1 show an increase of the Si and C content on the materials surfaces. The C content difference can be attributed to the organic molecules used for the surface modification. The Si increase is due to the APTS molecules treatment. Each APTS molecule introduces one Si atom to the surface. After surface modification the reference and modified samples exhibit a different Si content, the ratio being 1:2, which verifies the successful surface silanization. The coupling of GA to the surface was confirmed by a typical reddish color of the samples obtained after GA treatment. The APTS presence on a surface is known to be the prerequisite for the successful GA coupling. It has been shown in the literature [27, 38, 39] that GA has a very high affinity to APTS. On average it is assumed that one GA molecule docks to one APTS molecule.

After 3 days in SBF the Si content (data in Table 1) of the reference and the modified samples maintain the same level, with only a limited reduction of Si concentration in the as-fabricated sample. This suggests that the XPS analysis spot (1 mm^2) records Si signals from Bioglass® pellet areas that are not covered with HA layers or that some areas are not covered with HA layers thicker than about 10 nm. Both cases suggest a chemical stability of the silanized surface. It is suggested that the decrease of Si in the untreated sample was caused by silicate ion leaching, thus the lower reduction of Si in the surface modified samples should indicate a stable attachment of APTS molecules.

The fractions of C decrease significantly for both samples (Table 1). Interestingly, the modified samples exhibit after 3 days in SBF still a 50% higher C content as opposed to the reference probably due to organic molecules that are still coupled onto the surface. This fact not only confirms the stability of APTS attachment but also shows a firm adhesion of the GA molecules to the Bioglass® substrate.

4.2 Impact on bioactivity

SEM micrographs and XRD analysis confirm qualitatively a much more pronounced formation of HA for the heat-treated (80°C in aqueous solution for 4 hrs) and surface modified scaffolds (Figs. 2(b) and (c), Figs. 3(b) and (c), and Figs. 5(b) and (c)) as opposed to the sintered reference scaffold samples (Figs. 1(b) and (c), Fig. 5(a)). The obtained HA is Ca and P deficient as found by XPS and EDS analysis (Table 1 and Fig. 5, respectively).

Two mechanisms are suggested to contribute to the different HA formation rates. Firstly, Na, Ca and P ions are thought to be leached out of the glass structure during the aqueous heat-treatment at 80°C for 4 hrs and at pH 8 required for the surface modification. The fractions of these ions are significantly reduced as confirmed by EDS analysis in Fig. 4(c) and (f). The normally less soluble crystalline $Na_2Ca_2Si_3O_9$ phase is disrupted in its crystalline structure and therefore its solubility increased thus allowing a more rapid exchange of ions when immersed in the SBF solution. The XRD analysis (Fig. 5(b) and (c)) confirms that after 3 days immersion in SBF the crystalline phase has already disappeared as opposed to the non heat-treated reference (Fig. 5(a)).

In addition, SEM micrographs of heat-treated and surface modified samples have revealed a pronounced surface roughness at the micro scale (Figs. 2(a) and 3(a)) which is thought to be caused by ion leaching during the aqueous heat treatment. The increased surface roughness probably favors crystallization of HA when samples are immersed in SBF [40].

The comparable amounts of HA formed on heat-treated and surface modified samples indicate that the aqueous heat-treatment is likely to be the only reason for a faster HA formation for the reasons explained above. It can be concluded therefore that introducing APTS and GA molecules to the surface of a sintered Bioglass® substrate (both in porous scaffold and dense pellet form) does not influence the kinetics of HA formation upon immersion in SBF. This result is relevant considering the maintainance of the bioactive behaviour of Bioglass®-based scaffolds while enhancing their ability to bind bone tissue by the surface functionalization procedure introduced here. Indeed the growth of calcium phosphate coatings in the presence of biomolecules, such as albumin, fibronectin, has been shown to be substantially inhibited [41, 42]. Future research should consider the application of the strategy presented here on Bioglass®-based scaffolds for selective adhesion of relevant biomolecules.

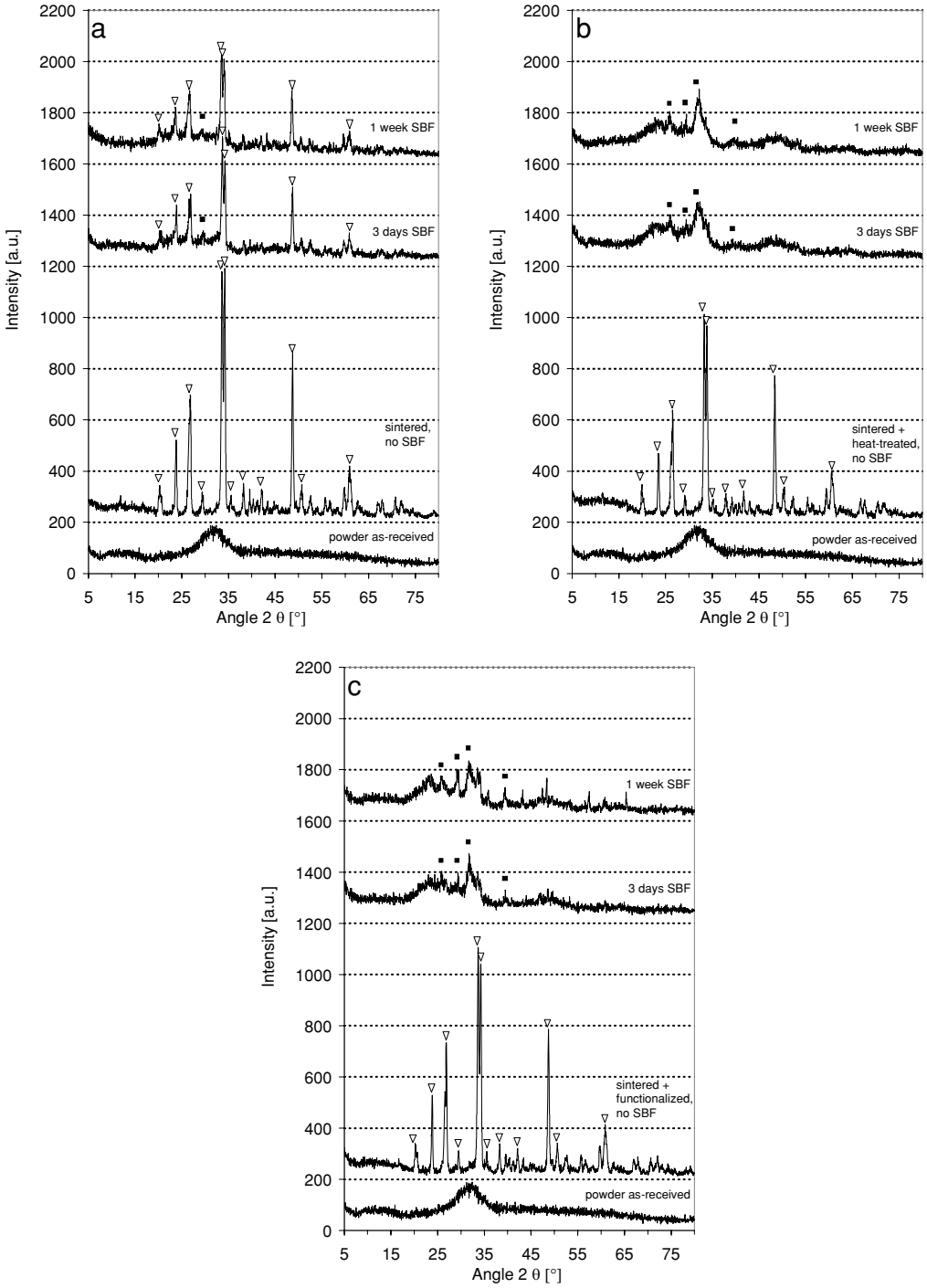

Fig. 5 XRD spectra of different scaffolds before and after 3 days and 1 week immersion in SBF: (a) sintered, (b) sintered and heat-treated, (c) sintered and functionalized. Triangles mark the $Na_2Ca_2Si_3O_9$ phase, solid squares the HA peaks. The heat-treated and modified samples exhibit only HA peaks and no indication of a $Na_2Ca_2Si_3O_9$ phase after 3 days in SBF

5 Conclusions

Surface functionalization of 45S5 Bioglass® scaffolds was carried out for the first time without using organic solvents. The process efficiency was verified by XPS analysis. The surface functionalized scaffolds are ready for protein immobilization and they can be used for protein release studies or to fabricate Bioglass® –protein hybrids.

The results of this study suggest that the aqueous heat treatment involved in the surface functionalization process leaches out Na, Ca and P ions from sintered Bioglass® scaffolds. This process affects the crystallinity of the sample,

inducing local surface roughness increment and, as a consequence thereof, it favors the formation of HA upon immersion in SBF. This simple aqueous heat treatment at 80°C can be applied to sintered Bioglass®-based scaffolds to remove or disrupt the stable crystalline $Na_2Ca_2Si_3O_9$ phase structure which is undesirable as it delays HA formation therefore impairing bioactivity.

Acknowledgment ARB acknowledges helpful discussions and inspiring conversations over the last few years with Professor Larry Hench (Imperial College London).

References

1. D. M. BRUNETTE, P. TENGVALL, M. TEXTOR and P. THOMSON, in "Titanium in Medicine - Material Science, Surface Science, Engineering, Biological Responses and Medical Applications" (Springer, 2001).
2. E. G. M. BUCCIANTINI, F. FABRIZIO CHITI, L. BARONI, J. FORMIGLI, N. ZURDO, G. TADDEI, C. M. RAMPONI, M. DOBSON and M. STEFANI, *Nature* **416** (2002) 507.
3. K. E. TANNER and W. BONFIELD, *Mater. World* **5** (1997) 18.
4. T. BOONTHEEKUL and D. J. MOONEY, *Curr. Opin. Biotechnol.* **14** (2003) 559.
5. B. W. G. SCHMIDMAIER, A. STEMBERGER, N. P. HAAS and M. RASCHKE, *J. Biomed. Mater. Res.* **58** (2001) 449.
6. S. A. GITTENS and H. ULUDAG, *J. Drug. Target.* **9** (2001) 407.
7. T. A. HOLLAND, Y. TABATA and A. G. MIKOS, *J. Controll. Rel.* **101** (2005) 111.
8. J. E. BABENSEE, L. V. MCINTIRE and A. G. MIKOS, *Pharma. Res.* **17** (2000) 497.
9. J. A. JANSEN, J. W. M. VEHOF, P. Q. RUHE, H. KROEZE-DEUTMAN, Y. KUBOKI, H. TAKITA, E. L. HEDBERG and A. G. MIKOS, *J. Controll. Rel.* **101** (2005) 127.
10. H. KESHAW, A. FORBES and. R. M. DAY, *Biomaterials* **26** (2005) 4171.
11. V. LUGINBUEHL, L. MEINEL, H. P. MERKLE and B. GANDER, *Europ. J. Pharm. Biopharm.* **58** (2004) 197.
12. P. Y. W. DANKERS, M. C. HARMSEN, L. A. BROUWER, M. J. A. VAN LUYN AND E. W. MEIJER, *Nature Mater.* **4** (2005) 568.
13. RUTH R. CHEN and D. J. MOONEY, *Pharm. Res.* **20** (2003) 1103.
14. A. H. ZISCH, M. P. LUTOLF and J. A. HUBBELL, *Cardiovasc. Pathol.* **12** (2003) 295.
15. J. L. DRURY and D. J. MOONEY, *Biomater.* **24** (2003) 4337.
16. A. ROSENGREN, S. OSCARSSON, M. MAZZOCCHI, A. KRAJEWSKI and A. RAVAGLIOLI, *Biomaterials* **24** (2003) 147.
17. K. REZWAN, A. R. STUDART, J. VÖRÖS and L. J. GAUCKLER, *J. Phys. Chem. B* **109** (2005) 14469.
18. P. M. BIESHEUVEL, P. STROEVE and P. A. BARNEVELD, *J. Phys. Chem. B* **108** (2004) 17660.
19. P. M. BIESHEUVEL, M. VANDERVEEN and W. NORDE, *J. Phys. Chem. B* **109** (2005) 4172.
20. R. D. WHITLEY, R. WACHTER, F. LIU and N. H. WANG, *J. Chromatogr* **465** (1989) 137.
21. K. REZWAN, L. P. MEIER, A. R. STUDART and L. J. GAUCKLER, *Biophys. J. in review* (2006).
22. M. LUNDQVIST, I. SETHSON and B. H. JONSSON, *Langmuir* **20** (2004) 10639.
23. J. BUIJS, M. RAMSTROM, M. DANFELTER, H. LARSERICSDOTTER, P. HAKANSSON and S. OSCARSSON, *J. Colloid Inter. Sci.* **263** (2003) 441.
24. M. HEULE, K. REZWAN, L. CAVALLI and L. J. GAUCKLER, *Adv. Mater.* **15** (2003) 1191.
25. H. H. WEETALL, *Trends Biotechnol.* **3** (1985) 276.
26. H. H. WEETALL, in "Covalent Coupling Methods for Inorganic Support Materials Methods in Enzymology" (Academic Press, 1976) p. 134.
27. R. A. WILLIAMS and H. W. BLANCH, *Biosensors and Bioelectronics* **9** (1994) 159.
28. H. H. WEETALL, *Biosensors and Bioelectronics* **8** (1993).
29. F. L. MI, Y. C. TAN, H. F. LIANG and H. W. SUNG, *Biomater* **23** (2002) 181.
30. R. F. S. LENZA, J. R. JONES, W. L. VASCONCELOS and L. L. HENCH, *J. Biomed. Mater. Res. Part A* **57A** (2003) 121.
31. Q. Z. CHEN and A. R. BOCCACCINI, *J. Biomed. Mater. Res. A* **77A** (2006) 445–457.
32. Q. Z. CHEN, I. D. THOMPOSON, and A. R. BOCCACCINI, *Biomaterials* **27** (2006) 2414.
33. T. KOKUBO, K. HATA, T. NAKAMURA and T. YAMAMURA, in "Bioceramics," edited by W. Bonfield and G. W. Hastings (Guildford Butterworth-Heinemain, London, 1991) p. 1339.
34. L. L. HENCH and T. KOKUBO, in "Handbook of Biomaterial Properties," edited by J. Black and G. Hastings (Chapman & Hall, London, 1998) p. 355.
35. T. KOKUBO, H. M. KIM and M. KAWASHITA, *Biomaterials* **24** (2003) 2161.
36. L. L. HENCH and J. WILSON, in "An Introduction to Bioceramics" (Word Scientific, London, 1999).
37. D. C. CLUPPER and L. L. HENCH, *J. Non-Cryst. Solids* **318** (2003) 43.
38. D. R. WALT and V. I. AGAYN, *TrAC Trends in Analyt. Chem.* **13** (1994) 425.
39. J. D. W. A. NANCI, L. PERU, P. BRUNET, V. SHARMA, S. ZALZAL and M. D. MCKEE, *J. Biome. Mater. Res.* **40** (1998) 324.
40. A. MERSMANN, in "Crystallization Technology Handbook." (New York, Marcel Dekker, Inc., 2001).
41. Y. LIU, P. LAYROLLE, J. DE BRUIJN, C. VAN BLITTERSWIJK and K. DE GROOT, *J. Biomed. Mater. Res.* **57** (2001) 327.
42. A. DO SERRO, A. FERNANDEZ and B. SARAMAGO, *J. Biomed. Mater. Res.* **49** (2000) 345.